Shock wave propagation in vibrofluidized granular materials

Kai Huang,* Guoqing Miao,† Peng Zhang, Yi Yun, and Rongjue Wei
State Key Laboratory of Modern Acoustics and Institute of Acoustics, Nanjing University, Nanjing 210093, People's Republic of China
(Received 21 October 2004; revised manuscript received 2 November 2005; published 18 April 2006)

Shock wave formation and propagation in vertically vibrated quasi-two-dimensional granular materials are studied by digital high speed photography. Steep density and temperature wave fronts form at the bottom of the granular layer when the layer collides with vibrating plate. Then the fronts propagate upwards through the layer. The temperature front is always in the transition region between the upward and downward granular flows. The effects of driving parameters and particle number on the shock are also explored.

DOI: 10.1103/PhysRevE.73.041302 PACS number(s): 45.70.Mg, 46.40.−f

Granular materials are ubiquitous in nature and play an important role in industries and in our daily lives [1]. Due to their noncohesive, strongly dissipative properties, granular materials behave differently from usual solids, liquids, and gases. When vibrated vertically, the state of a granular material changes from solid, to liquid, to gas, as the input energy increases. These states and the phase transitions between them have been studied experimentally and theoretically [2]. Fluidized granular materials show many interesting phenomena, such as surface patterns [3], oscillons [4], convection [5], size and density segregation [6], clusters [7], heap formation [8], and transport [9], etc. Recently sound propagation in vibrofluidized granular media has attracted much interest, because it coexists with most of the above phenomena and is not well understood. Wave propagation in dilute granular materials, which we study here, is different from that in confined granular materials. Theoretical [10] and experimental [11] studies show that sound in close packed granular materials propagates mainly through force chains. Computer simulations indicate that there exist density and pressure waves in dilute granular materials under vertical vibrations [12]. Recently, time-independent shocks in granular flow past an obstacle have been observed in experiments and compared with simulation results [13]. Similarly, when an object is moving through vibrofludized granular media, a wake (Mach cone), whose angle follows the Mach relation, appears [14]. Moreover, the formation and propagation of shocks in vibrofluidized granular materials have been studied by molecular dynamic simulations and numerical analyses of continuum equations [15] based on the kinetic theory of nonuniform gases [16]. To explore dynamic behaviors of fluidized granular materials, various noninvasive experimental methods have been introduced [17–20]. Experimental results indicate that the properties of vibrofluidized granular materials will be highly time dependent, if the driving frequency is relatively low. The variation of granular temperature in one oscillation cycle has recently been measured by diffusion wave spectroscopy [21]. However experimental studies of wave propagations in vibrofluidized granular materials are scarce. In this paper, we use high speed photography to explore shock formation and propagation in vertically vibrated, quasi-two-dimensional granular materials.

The experiment is conducted with a rectangular container mounted on the vibrating exciter (Brüel & Kjær 4805), which is controlled by a function generator (type HP 3314A). We use steel spheres with diameter $d=4$ mm and density $\rho=7900\ \mathrm{kg/m^3}$. The container is made up of two parallel glass plates with length $l=90$ mm, height $h=280$ mm and separated by $w=4.1$ mm vertically fixed in a Plexiglass bracket. The total particle number N, the driving frequency f, and the nondimensional acceleration $\Gamma=4\pi^2 f^2 A/g$ (A is the driving amplitude and g the gravitational acceleration) are used as control parameters. The whole experiment is performed in the presence of air. A high speed camera (Redlake MASD MotionScope PCI 2000sc) is used to record the movements of all spheres. A frequency multiplication and phase lock circuit is used to generate external trigger signals for the camera. The acquisition rate is $N_p\times f$ with multiple number $N_p=25$. Every recorded image [$22d$(length) $\times 30d$(height)] contains the locations of all the particles. An image technique [22] is used to track the locations of all particles. We use the vibrating container as the reference frame in image processing. To get rid of the influence of side walls, we choose a region of width $l_s=18d$ at the center of each image for statistics. Statistical results with other width $(16d,10d)$ yield the same results as with the $18d$ width. In addition, every chosen region is divided vertically into a number of strips, each with a height $h_s=1d$ and indicated by 1,2,…. from bottom to top. An assembly average is performed over 600 cycles at N_p phase points in each cycle. The packing fraction $\nu(jh_s,k\Delta t)=N_s(jh_s,k\Delta t)V_p/V_s$ is the ratio of the volume that particles in a strip occupy to the volume of the strip V_s, in which $V_p=\pi d^3/6$ is the volume of a particle, $V_s=l_s h_s w$ is the volume of a strip, and $N_s(jh_s,k\Delta t)$ is the number of particles in jth strip at time $k\Delta t$, where $\Delta t=1/(N_p f)$. For brevity, we omit the units of space and time and use $\nu(j,k)$ instead of $\nu(jh_s,k\Delta t)$ hereafter. Granular temperature is defined by $T(j,k)=\Sigma_{n=1}^{N_s}\frac{1}{2}|\mathbf{v}_n-\mathbf{v}_b(j,k)|^2/N_s$, in which N_s is the number of particles at height j and phase point k, $\mathbf{v}_n$ is the velocity vector of the nth particle, and the background velocity is $\mathbf{v}_b(j,k)=\Sigma_{n=1}^{N_s}\mathbf{v}_n/N_s$.

As Γ increases to and beyond 1, the granular layer fluidizes from top to lower parts, and the density fluctuation or

*Electronic address: huangkai1996@nju.org.cn
†Electronic address: miaogq@nju.edu.cn

 ©2006 The American Physical Society

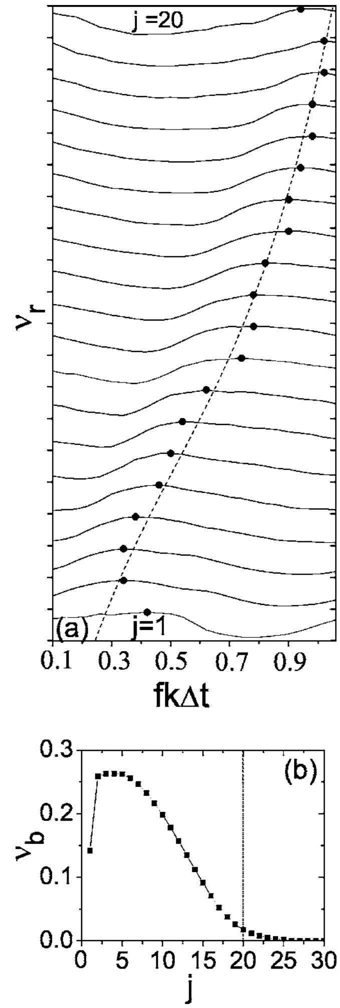

FIG. 1. (a) Time-space profiles of packing fraction ν_r from $j=1$ to 20. Solid circles represent peak-value points of density at each strip, dashed line is the polynomial fitting of peak values with time. $fk\Delta t=0$ corresponds to the time when the plate reaches its minimum height; (b) background packing fraction ν_b versus height j. Parameters are $f=15$ Hz, $\Gamma=5$, and $N=150$. The height of peak-value point at each strip is set at 90% of total height of that strip.

density wave defined by $\nu_r(j,k)=\nu(j,k)-\nu_b(j)$ [the background packing fraction $\nu_b(j)=\Sigma_{k=1}^{N_p}\nu(j,k)/N_p$] appears in the layer [as shown in Fig. 1(a)]. The density at the bottom of the layer reaches its maximum at $fk\Delta t=0.4$, where $fk\Delta t$ is the normalized time. Figure 1(a) shows the time-space profile of density wave. The fitting curve of density peaks of all the strips indicates that the density wave propagates upward with a nonuniform velocity, faster below than above $j=3$, and is in agreement with the results obtained from molecular dynamic simulations [12]. The wave distorts as it moves upward. It is well known that in ordinary gas the distorted wave will evolve into a shock wave as it propagates. The calculation of Mach number Ma indicates that there exists shock waves in our experiment. As a supersonic granular flow encounters an impenetrable plate, velocities of the particles (relative to the plate) near the plate abruptly decrease to about zero, but those of the undisturbed particles are still unchanged. This results in a normal shock formation near the

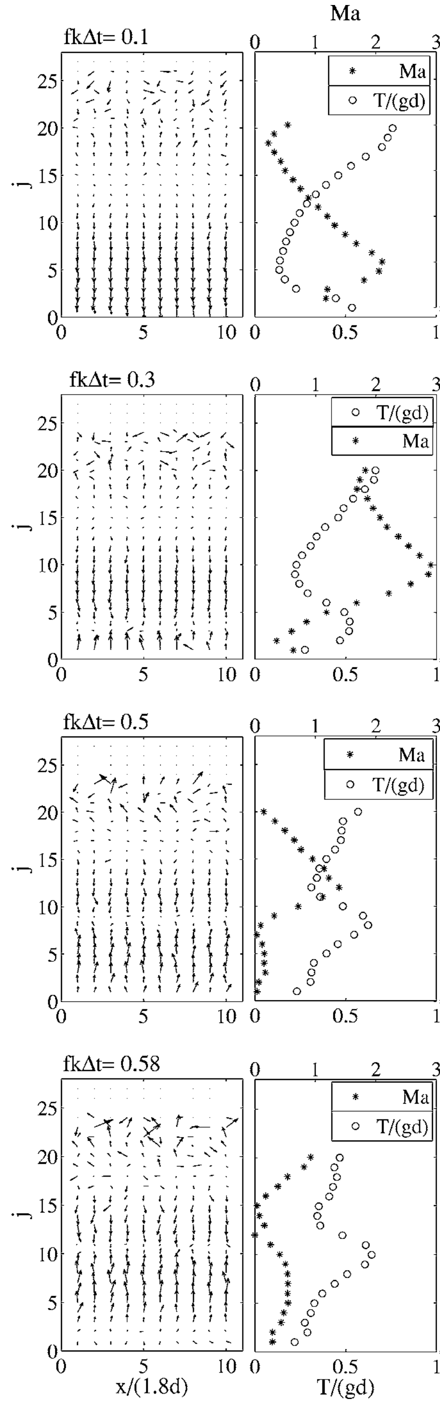

FIG. 2. Two dimensional background velocity field (left column), Mach number Ma (asterisk), and scaled temperature (open circle) (right column) as a function of height (right) at four different times. At time $fk\Delta t=0.5$ the plate is at its highest position. Parameters here are the same as those in Fig. 1.

plate. Then, this shock wave leaves plate and propagates upward. We only plot density profiles below $j=20$, because above that height the number of particles captured is too small for accurate statistics [Fig. 1(b)].

In the experiment, the shock is identified in a transition region between disturbed and undisturbed regions, where the Mach number increases from its minimum (<1) in the dis-

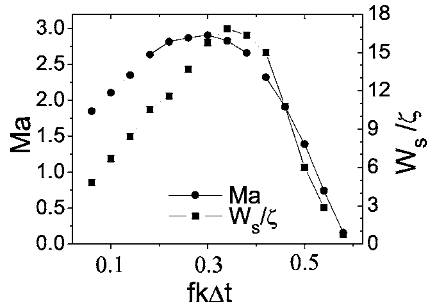

FIG. 3. The peak value of Mach number and the normalized shock width W_s/ζ as a function of time. The mean free path of particles is $\zeta(j,k)=\sqrt{\pi/8}/[n(j,k)\pi d^2]$, where $n(j,k)=\nu(j,k)/V_p$ is the number density. The shock begins to form at $fk\Delta t=0.1$ and disappear at $fk\Delta t=0.5$. Shock width W_s/ζ reaches its maximum value 16.8 at $fk\Delta t=0.34$. Parameters here are the same as those in Fig. 1.

turbed region to the maximum (>1) in the undisturbed region. The shock width W_s is defined as the width of the transition region and the shock location is identified as the center of the region. The Mach number is defined by

$$Ma=\left|\frac{v_{bn}-v_p}{c}\right|, \tag{1}$$

where v_{bn} is the vertical component of $\mathbf{v}_b$, v_p is the velocity of the plate, and c is the speed of sound estimated with a formula derived from kinetic theory [15,23]

$$c=\sqrt{T\chi\left(1+\chi+\frac{\nu}{\chi}\frac{\partial\chi}{\partial\nu}\right)}, \tag{2}$$

in which $\chi=1+2(1+e)\nu[1-(\nu/\nu_{max})^{4\nu_{max}/3}]^{-1}$, the restitution coefficient e is chosen to be 0.85 (similar results are obtained with e varying from 0.75 to 0.9) and $\nu_{max}=NV_p/(2h_{cm}lw)=0.57$ is the maximum packing fraction [22]. The height h_{cm} of the center of mass at rest is calculated by

$$h_{cm}=\frac{n_b d}{2N}[(1-\sqrt{3}/2)n_h+(\sqrt{3}/2)n_h^2]+\frac{n_0 d}{2N}(1+\sqrt{3}n_h), \tag{3}$$

in which $n_b=l/d-0.5$ is the average number of particles per strip, $n_h=\mathrm{int}(N/n_b)$ is the number of full strips, and $n_0=N-n_h n_b$ is the particle number at the highest strip [22]. We investigate the propagation of the shock by examining the two dimensional background velocity field, the distribution of granular temperature and Mach number at four times in one cycle (shown in Fig. 2). The two dimensional background velocity field is obtained by dividing each of the selected region into 10 columns ($1.8d$ width each) and averaging for the velocities of all the particles in column $x/(1.8d)$, strip j, and time k. The maximum Mach number in the shock and the normalized shock width W_s/ζ as functions of time are shown in Fig. 3.

At $fk\Delta t=0.1$, the plate moves upward with $v_p=0.306$ m/s and begins to collide with the granular layer. Particles at lower strips begin to be compressed by the collision. In the mean time, most of the particles in the undisturbed region are still falling towards the plate with supersonic speed. This results in the formation of a shock. In the shock region the Mach number increases with height and reaches a maximum value of 2.11 at $j=5$. The particle velocities are randomized by collisions and the granular temperature decreases with height in this region.

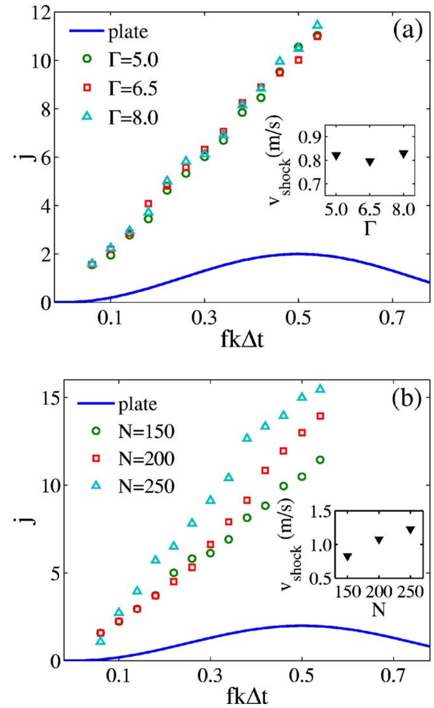

FIG. 4. (Color online) Shock location as a function of time with different Γ (a) and N (b). Shock speed as functions of Γ and N are shown separately in the insets of (a) and (b). f and N are fixed at 20 Hz and 150 in (a) and f and Γ are fixed at 20 Hz and 8 in (b). Solid line represents the vibration of the plate.

At $fk\Delta t=0.3$, the plate moves upward with $v_p=0.495$ m/s. The granular layer continues to be compressed on the plate, more and more particles come into the compressed region, resulting in the propagation of the shock up through the layer and the increase of the shock width W_s/ζ. In the shock region, the Mach number increases with height and reaches its maximum ($Ma=2.91$) at $j=10$ [Fig. 3(b)]. A temperature peak appears at $j=3$ which is the bottom of shock region and is also the transition region between upward and downward granular flows.

At $fk\Delta t=0.5$, the plate reaches its maximum height. The granular layer leaves the plate and flies freely. The shock propagates upward, with the maximum Mach number decreasing to 1.39 at $j=12$. The variation of shock width (Fig. 3) indicates that the shock steepens dramatically and is almost fully developed, as it is propagating upward at this time. The steeping temperature wave front propagates upward to $j=10$.

After $fk\Delta t=0.5$, the plate begins to move downward. The maximum Mach number in the shock region decreases. At $fk\Delta t=0.58$, the shock disappears, because the maximum Mach number at $j=13$ damps to be less than unity. The temperature wave front continues to propagate upward until it disappears in the dilute region of the layer. Then the granular layer is ready for the next collision with the plate.

To investigate how changing Γ and N affect the shock, we perform the experiment with Γ from 5 to 8 and N from 150 to 250. As Γ increases, the velocity of granular layer relative to the plate increases, resulting in the increase of maximum Mach number and the speed of shock. On the other hand, as Γ increases, the average number density decreases (particles expand to fill more space), and this results in a decrease of the propagating velocity of the wave [24]. As a result the total effect of these two opposite effects make the velocity of shock change little with the change of Γ [Fig. 4(a)]. As the total number of particles increases from 150 to 250 (the layer depth from $7d$ to $11d$) with driving parameters fixed, the average number density increases. The speed of the shock increases monotonously with the increase of number density. This is due to the fact that the perturbation is mainly transmitted through collisions between particles. The increase of granular density leads to the decrease of the mean free path, which in turn results in particles colliding more frequently and in the energy transmitting faster.

Our experimental results are in qualitatively agreement with the theoretical one of Bougie *et al.* [15]. Quantitatively, the maximum Mach number and shock speed of [15] is larger than those of our experiment. One of the reasons for the difference is that the amplitude of the vibrating plate in [15] is more than five times larger than in our experiment, which leads to larger velocity of granular layer relative to vibrating plate. Therefore, the maximum Mach number and the shock speed in the theory is larger than in our experiment. Another reason is the difference in granular density. The maximum packing fraction (0.64) [25] in the three-dimensional system of [15] is larger than in the quasi-two-dimensional system (0.57) of ours. Also, the packing fraction in [15] is larger than in the experiment. Another is the neglect of friction in Bougie *et al.*'s work [15]. According to the simulation study by Moon *et al.* [26], friction leads to the decrease of shock speed.

In conclusion, we prove the existence of a shock wave in vibrofuidized granular materials experimentally. The shock forms as particles collide with vibrating plate and propagates upward with a steep temperature front in the transition region between upward and downward granular flows. The velocity of the shock depends on the velocity of the plate when it collides with granular layer and the number density of granular layer. Our experiment provides a better basis for further theoretical studies of granular materials and is helpful for the understanding of phenomena in vibrofluidized granular materials such as surface instabilities, convection, and energy transfer, etc.

The authors appreciate James T. Jenkins for critical reading of the manuscript. This work was supported by the Special Funds for Major State Basic Research Projects, National Natural Science Foundation of China through Grant No. 10474045 and No. 10074032, and by the Research Fund for the Doctoral Program of Higher Education of China under Grant No. 20040284034.

[1] H. M. Jaeger and S. R. Nagel, Rev. Mod. Phys. **68**, 1259 (1996).

[2] A. Goldshtein, M. Shapiro, L. Moldavsky, and M. Fichman, J. Fluid Mech. **287**, 349 (1995); A. Goldshtein and M. Shapiro, J. Fluid Mech. **282**, 75 (1995).

[3] F. Melo, P. Umbanhowar, and H. L. Swinney, Phys. Rev. Lett. **72**, 172 (1994); F. Melo, P. B. Umbanhowar, and H. L. Swinney, Phys. Rev. Lett. **75**, 3838 (1995); E. Clement, L. Vanel, J. Rajchenbach, and J. Duran, Phys. Rev. E **53**, 2972 (1996); S. Luding, E. Clement, J. Rajchenbach, and J. Duran, Europhys. Lett. **36**, 274 (1996); C. Bizon, M. D. Shattuck, J. B. Swift, W. D. McCormick, and H. L. Swinney, Phys. Rev. Lett. **80**, 57 (1998).

[4] P. B. Umbanhowar, F. Melo, and H. L. Swinney, Nature (London) **382**, 793 (1996); S. C. Venkataramani and E. Ott, Phys. Rev. E **63**, 046202 (2001).

[5] J. B. Knight, E. E. Ehrichs, V. Y. Kuperman, J. K. Flint, H. M. Jaeger, and S. R. Nagel, Phys. Rev. E **54**, 5726 (1996).

[6] J. B. Knight, H. M. Jaeger, and S. R. Nagel, Phys. Rev. Lett. **70**, 3728 (1993); N. Burtally, P. J. King, and M. R. Swift, Science **295**, 1877 (2002).

[7] S. Miller and S. Luding, Phys. Rev. E **69**, 031305 (2004).

[8] M. Faraday, Philos. Trans. R. Soc. London **121**, 299 (1831); P. Evesque and J. Rajchenbach, Phys. Rev. Lett. **62**, 44 (1989).

[9] K. Huang, G. Q. Miao, and R. J. Wei, Int. J. Mod. Phys. B **17**, 4222 (2003).

[10] W. Gregor and H. Rumph, Int. J. Multiphase Flow **1**, 753 (1975); E. Somfai, J. N. Roux, J. H. Snoeijer, M. van Hecke, and W. van Saarloos, Phys. Rev. E **72**, 021301 (2005); V. Tournat, V. E. Gusev, and B. Castagnède, Phys. Rev. E **66**, 041303 (2002).

[11] C. H. Liu and S. R. Nagel, Phys. Rev. Lett. **68**, 2301 (1992); C. H. Liu and S. R. Nagel, Phys. Rev. B **48**, 15646 (1993).

[12] K. M. Aoki and T. Akiyama, Phys. Rev. E **52**, 3288 (1995).

[13] E. C. Rericha, C. Bizon, M. D. Shattuck, and H. L. Swinney, Phys. Rev. Lett. **88**, 014302 (2002).

[14] P. Heil, E. C. Rericha, D. I. Goldman, and H. L. Swinney, Phys. Rev. E **70**, 060301(R) (2004).

[15] J. Bougie, S. J. Moon, J. B. Swift, and H. L. Swinney, Phys. Rev. E **66**, 051301 (2002).

[16] A. Goldthtein, M. Shapiro, and C. Gutfinger, J. Fluid Mech. **316**, 29 (1996).

[17] X. Yang, C. Huan, D. Candela, R. W. Mair, and R. L. Walsworth, Phys. Rev. Lett. **88**, 044301 (2002); C. Huan, X. Yang, D. Candela, R. W. Mair, and R. L. Walsworth, Phys. Rev. E **69**, 041302 (2004); X. Yang and D. Candela, Phys. Rev. Lett. **85**, 298 (2000).

[18] N. Menon and D. J. Druian, Science **275**, 1920 (1997); N. Menon and D. J. Durian, Phys. Rev. Lett. **79**, 3407 (1997); R. Ojha, N. Menon, and D. J. Durian, Phys. Rev. E **62**, 4442 (2000).

[19] J. C. Tsai, W. Losert, G. A. Voth, and J. P. Gollub, Phys. Rev.

E **65**, 011306 (2001); J. C. Tsai, G. A. Voth, and J. P. Gollub, Phys. Rev. Lett. **91**, 064301 (2003); R. P. Ojha, P. A. Lemleux, P. K. Dixon, A. J. Liu, and D. J. Durian, Nature (London) **427**, 521 (2004).

[20] G. T. Seidler, G. Martinez, L. H. Seeley, K. H. Kim, E. A. Behne, S. Zaranek, B. D. Chapman, S. M. Heald, and D. L. Brewe, Phys. Rev. E **62**, 8175 (2000).

[21] P. K. Dixon and D. J. Durian, Phys. Rev. Lett. **90**, 184302 (2003).

[22] R. D. Wildman, J. M. Huntley, J.-P. Hansen, D. J. Parker, and D. A. Allen, Phys. Rev. E **62**, 3826 (2000); S. Warr, G. T. H. Jacques, and J. M. Huntley, Powder Technol. **81**, 41 (1994); R. D. Wildman and J. M. Huntley, Powder Technol. **113**, 14 (2000); S. Warr, J. M. Huntley, and G. T. H. Jacques, Phys. Rev. E **52**, 5583 (1995).

[23] S. B. Savage, J. Fluid Mech. **194**, 457 (1988); P. K. Haff, J. Fluid Mech. **134**, 401 (1983); J. Jenkins and M. Richman, Arch. Ration. Mech. Anal. **87**, 355 (1985); J. T. Jenkins and S. B. Savage, J. Fluid Mech. **130**, 187 (1983).

[24] S. Harada, S. Takagi, and Y. Matsumoto, Phys. Rev. E **67**, 061305 (2003).

[25] R. Ojha, N. Menon, and D. J. Durian, Phys. Rev. E **62**, 4442 (2000).

[26] S. J. Moon, J. B. Swift, and H. L. Swinney, Phys. Rev. E **69**, 031301 (2004); S. J. Moon, J. B. Swift, and H. L. Swinney, Phys. Rev. E **69**, 011301 (2004).